Metallurgical and Materials Data 2, no. 4 (2024): 119-129

Publisher: Association of Metallurgical Engineers of Serbia

Metallurgical and Materials Data

www.metall-mater-data.com

Comparative analysis of cystine and cysteine as green corrosion inhibitors of aluminium alloy AA7075-T6

Jovanka Pejić[1]*, Dunja Marunkić[1], Aleksandar Jovanović[2], Nikola Vuković[2], Bojana Radojković[1]

[1]*Institute of Chemistry, Technology and Metallurgy, University of Belgrade, Njegoševa 12, 11000 Belgrade, Serbia*

[2]*Institute for Technology of Nuclear and Other Mineral Raw Materials, Boulevard Franše d'Eperea 86, 11000 Belgrade, Serbia*

ARTICLE INFORMATION:

https://doi.org/10.56801/MMD43

Received: 13 December 2024
Accepted: 01 February 2025

Type of paper: Research paper

ABSTRACT

Cystine and cysteine as green corrosion inhibitors of the 7075 aluminium alloy in 0.1 M NaCl solution were analysed and compared. The inhibitive efficiency of the inhibitors was analysed by applying linear polarization resistance (LPR) and electrochemical impedance spectroscopy (EIS) methods. Different concentrations of both inhibitors in NaCl solution were tested under different temperatures and times to determine the corrosion kinetic and thermodynamic parameters. Optical microscopy (OM) and scanning electron microscopy (SEM) were used for analysis of the aluminium alloy surface before and after the electrochemical measurements. The hydrophilicity of the alloy surface with tested inhibitors was compared by applying contact angle measurements. The results showed that cystine and cysteine are effective corrosion inhibitors, with different characteristics and duration of protection on the tested aluminium alloy. Cysteine showed better efficiency for short-term applications while cystine provided more stable protection over a longer period.

Keywords: aluminium alloys, AA7075, green corrosion inhibitors, EIS, SEM/EDS.

1. Introduction

Aluminium alloy from the 7xxx series (7075 aluminium alloy) is known for its high strength, low density, good thermal properties and polishability. They are widely used in the automotive and aviation industries (Nakata et al. 2000). The 7075 alloy contains zinc as the main alloying element and magnesium and copper in smaller amounts (Vargel 2004).

Different heat treatments are applied to aluminium alloys, such as AA7075, to achieve improved mechanical properties (Vargel 2004). Aluminium alloy 7075 is usually used after one- or two-step ageing. During one-step ageing (T6 thermal treatment), Guinier-Preston (GP) zones and semi-coherent precipitates η′ are formed, ensuring the alloys maximum strength. In two-step ageing (T73 heat treatment), the 7075 alloy acquires a microstructure that provides high resistance to stress corrosion cracking, with a certain reduction in the strength (L. L. Wei et al. 2015; M. O. Speidel 1972). After one-step and two-step ageing, aluminium alloys have relatively low corrosion resistance, especially to pitting corrosion, so it is important to develop a procedure for their protection.

Aluminium alloys form a protective oxide film (Al_2O_3) on their surface in an atmospheric environment, giving them good corrosion resistance. However, the corrosion resistance of the aluminium alloys is easily degraded in acidic and alkaline environments. Specifically, the presence of chloride ions (for example in the sea atmosphere) reduces the corrosion resistance of the aluminium alloys (Nakata et al. 2000) and causes localized types of corrosion, such as pitting, intergranular, stress corrosion cracking, and exfoliation corrosion (Andreatta, Terryn, and De Wit 2004; V.S Sinjavskij, V.D. Valjkov 1986).

Among various corrosion protection strategies, corrosion inhibitors are the simplest and most economical approach used in the industry. By adding an inhibitor to the corrosion medium, the corrosion rate is reduced to an acceptable level (Constable, Curzons, and Cunningham 2002; Swatloski et al. 2002).

Compounds containing hexavalent chromium which are very effective in metal corrosion protection, are restricted in the European Union due to their high toxicity and carcinogenicity (Directive (EU) 2022/431; Costa and Klein 2006), so there is a wide research effort to find adequate green (eco-friendly) inhibitors. Amino acids as green corrosion inhibitors have shown great potential in the corrosion protection of steel, copper alloys and aluminium alloys, besides other green organic acids.

Cysteine is a very common amino acid found in many proteins and enzymes, such as keratin in hair. The chemical formula of cysteine is $C_3H_7NO_2S$. Cysteine contains amino (–NH_2), carboxyl (–COOH) and thio (–SH) groups and can form complexes with many metals. In addition, cysteine can form bonds with metal surfaces, through all three mentioned functional groups, allowing a wide range of possibilities for corrosion protection (Costa and Klein 2006).

* Corresponding authors.
E-mail address: jovanka.kovacina@ihtm.bg.ac.rs (Jovanka Pejić).

The cystine is an amino acid and it is present in digestive enzymes, cells of the immune system, skin and hair, but it is most often obtained from two molecules of cysteine. The formula of cystine (SCH2CH(NH2) CO2H)2 shows that it has two carboxyl groups, two amino groups and a disulphide bond.

Corrosion inhibition properties of cysteine have been tested on several metals. It has been used as a corrosion inhibitor on aluminium alloys Al-Mn (AA3003) (El Ibrahimi et al. 2018), carbon steel (B. Zhang et al. 2015), as well as on copper alloys Cu-30Ni (Saifi et al. 2010), Cu5-Zn-5Al-1Sn (Shinato et al. 2019) and Cu(111) monocrystal (Milošev et al. 2013). While cysteine itself has been extensively studied, its derivative, cystine, has been less investigated. Cystine has been tested only on mild steel (Morad 2008; B. A. ABD-E1-NABEY 1985) and iron (Hluchan, et al. 1988), in acidic environments. Zhang (B. Zhang et al. 2015) showed that under acidic conditions cystine is more effective than cysteine. Cysteine potentially offers greater stability due to its two groups (-NH and -COOH), which can be stably adsorbed, while cysteine also has a -SH group which, although also adsorbable, is prone to oxidation and disulphide bond formation (P. Zhang et al. 2023).

This work represents an innovative contribution to the study of green corrosion inhibitors in neutral environments, especially in NaCl solution, which is relevant for aluminium and its alloys, which are often exposed to chloride solutions. While cysteine is an effective corrosion inhibitor in neutral environments, there is a lack of data on the behaviour of cystine in the same conditions.

In this work, a comparison of cystine with cysteine was performed to clarify its inhibitive properties. Given that aluminium and its alloys are widely used materials in industry and everyday use, the results of the research have practical applications. The advantage of cystine is its stability and ability to adsorb efficiently, which may lead to the development of new and more effective corrosion inhibitors for aluminium alloys in neutral environments.

2. Experiment

2.1. Materials

The chemical composition of the 7075 aluminium alloy was determined using the XRF (Olympus Vanta C Series Handheld XRF Analyzer) method. The tested specimens were made of the aluminium alloy 7075-T6 (one-step ageing). This thermal condition contributes to high strength and good mechanical properties and low corrosion properties. Before testing, specimens were wet polished with abrasive papers (SiC) up to 1500 grit, degreased with ethanol, washed with distilled water and dried.

2.2. Solution preparation

Experiments were performed in 0.1 M NaCl solution, without and in the presence of corrosion inhibitors. Different concentrations of the inhibitors were tested in the range from 0.03 mM to 0.1 mM. The chemicals used for the preparation of the solutions are NaCl (p.a. grade, Sigma Aldrich), cysteine (≥98 %, Sigma Aldrich), cystine (99 %, Across Organics) and bi-distilled water (high purity water 18 MΩ cm resistance, produced using Milli-Q Water Purification Systems).

The two-dimensional (2D) structures of cystine and cysteine are shown in Figure 1.

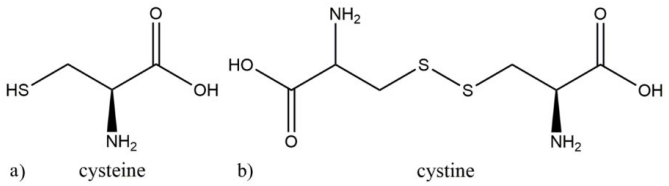

Fig. 1. Two-dimensional (2D) chemical structure: a) cysteine and b) cysteine.

2.3. Linear Polarisation Resistance (LPR)

The linear polarization technique was used to determine the value of polarization resistance (R_p) of the aluminium alloy specimens (AA7075) in 0.1 M NaCl solution, without and in the presence of investigated corrosion inhibitors (cysteine and cystine). The R_p value is inversely proportional to the corrosion current density (j_{corr}) and the corrosion rate (C_R). The aluminium alloy specimen in the solution was polarized in a narrow potential range (±15 mV) relative to the corrosion potential (E_{corr}), starting from the cathodic to the anodic region, and the corresponding value of current density (j) was registered. The applied sweep rate was 0.167 mV/s. The value of R_p is determined as the slope of the experimental E–j curve, at the corrosion potential. The measurements were carried out by applying a potentiostat/galvanostat/ZRA GAMRY 1010E device, in the three compartment electrochemical cell with volume of 150 cm^3. The working electrode was the aluminium alloy (surface area 1 cm^2), the counter electrode was a Pt-mesh, and the reference electrode was a saturated calomel electrode (SCE).

2.4. Electrochemical Impedance spectroscopy (EIS)

Electrochemical impedance spectroscopy measurements were performed in a conventional three-electrode electrochemical cell in a 0.1 M NaCl solution, without and in the presence of investigated corrosion inhibitors. For all electrochemical experiments, the same electrochemical cells and electrodes, and the same electrochemical device as in the LPR method were used. After establishing a relatively stable E_{corr}, a sinusoidal voltage signal of ±10 mV was applied relative to the corrosion potential in the frequency range from 100 000 to 0.01 Hz. The obtained results were analysed using Gamry Echem Analyst software.

2.5. SEM/EDS analysis

Microstructural analyses of 7075 aluminium alloy specimens before and after electrochemical testings were performed using scanning electron microscopy (SEM). Before analysis, specimens were polished with abrasive paper with a grain size of up to 1500, and then polished using Al_2O_3 polishing paste with grain sizes up to 0.3 μm. The specimens were cleaned in a water ultrasonic bath for 20 min and then degreased with ethanol. Analysis was performed using a scanning electron microscope JEOL JSM-6610LV, equipped for EDS measurements.

2.6. Optical microscopy

An optical microscope was used to study the morphological changes on the surface of the aluminium alloy. A macro view of the surface of 7075 aluminium alloy, after immersion for 10 days in 0.1 M NaCl solution, without and in the presence of investigated corrosion inhibitors (cysteine and cystine), was recorded using an optical microscope Delta Optical Smart 5MP PRO digital USB microscope.

2.7. Contact angle measurements

The contact angle measurements on the surface of the aluminium alloy specimens were performed after 24 h immersion in a 0.1 M NaCl solution, without and in the presence of investigated corrosion inhibitors (cysteine and cystine). This method allows visualization of the effect of the NaCl solution with the presence of corrosion inhibitors. After immersion, the aluminium specimens were removed, rinsed with bi-distilled water and dried. The measurement was performed at room temperature, by placing a drop of bi-distilled water on the surface of the aluminium alloy. The contact angle was recorded using a Delta Optical

Smart 5MP PRO digital USB microscope, and the value of the contact angle was determined using Image-Pro Plus 4.0 image analysis software (Media Cibernetics Inc., Rockville, MD, USA).

2.8. Kinetics and Thermodynamics analysis

Physically adsorbed inhibitors interact quickly but are easily desorbed from the metal surface. In contrast, chemically adsorbed inhibitors involve the sharing or transfer of electrons between the inhibitor and the metal making the inhibitors more effective.

Physically adsorbed inhibitors lose their effectiveness at higher temperatures and require a higher concentration, while the effectiveness of chemisorbed inhibitors increases to the point of molecular decomposition.

The kinetic parameters, as activation energy (Ea), can be obtained based on the Arrhenius equation (Nakomčić 2016):

$$j_{corr} = A \cdot exp\left(-\frac{Ea}{RT}\right) \quad (1)$$

Where: j_{corr} is the corrosion current density which is directly proportional to the corrosion rate (C_R), A is the pre-exponential factor, E_a is the activation energy, R is the universal gas constant, and T is the temperature.

Another form of the Arrhenius equation is (Nakomčić 2016):

$$j_{corr} = \frac{RT}{Nh} \cdot \exp\left(-\frac{\Delta H^{\circ}}{RT}\right) \cdot \exp\left(-\frac{\Delta S^{\circ}}{R}\right) \quad (2)$$

Where: ΔH° is activation enthalpy, ΔS° is activation entropy, h is Plancks constant and N is Avogadros number.

The inhibitor adsorption constant (Kads) can be determined based on the adsorption isotherm. The adsorption isotherm describes a relationship between the surface coverage of the inhibitor and its concentration in the solution. Mathematical forms of adsorption isotherms are used to analyze the ability of corrosion inhibitors to adsorb on the metal surface as a function of concentration (M.G. Fontana 1987). To obtain an isotherm, it is necessary to determine the degree of surface coverage (θ) in relation to the inhibitor concentration. Values of θ can be determined by electrochemical impedance spectroscopy, and are calculated as inhibition efficiency, IE(%)/100.

To determine the inhibitor adsorption, it is important to apply isotherm which describes the process the best. The Langmuir isotherm is given by the following equation (A. El-Haleem et al. 2013):

$$\frac{\theta}{1-\theta} = K \cdot c \quad (3)$$

Where: K is the Langmuir adsorption constant, and c is the molar concentration of the inhibitor.

The Langmuir isotherm can also be represented in the form (A. El-Haleem et al. 2013; Tawfik 2015):

$$\frac{c}{\theta} = \frac{1}{K} + \text{const} \quad (4)$$

Thermodynamic parameters of inhibitor adsorption include standard Gibbs energy of adsorption (ΔG_{ads}°), standard enthalpy (ΔH_{ads}°) and standard entropy (ΔS_{ads}°). These parameters provide information on the spontaneity of adsorption and the thermodynamic stability of the inhibitor on the metal surface. Also, they indicate changes in energy and energy distribution in the process of corrosion or corrosion inhibition, which is crucial for the selection and application of adequate corrosion inhibitors.

The equilibrium standard Gibbs energy is related to the Langmuir adsorption constant (K) through the following equation (A. El-Haleem et al. 2013):

$$K = \frac{1}{55.5} \exp\left(\frac{-\Delta G^{\circ}}{RT}\right) \quad (5)$$

Where the value 55.5 represents the concentration of water in the solution expressed in mol/l.

The fundamental thermodynamic relation between the standard adsorption Gibbs energy and equilibrium constant is (Kokalj 2023):

$$K_{ads} = \exp\left(\frac{-\Delta G^{\circ}}{RT}\right) \quad (6)$$

The temperature dependence of the adsorption constant is calculated using the Vanthoff equation (Uhlig and Revie 1985):

$$\ln K_{ads} = -\frac{\Delta H^{\circ}_{ads}}{RT} + \text{const} \quad (7)$$

3. Results and discussion

3.1. Materials

The chemical composition of AA7075 determined using XRF method is given in Table 1.

Table 1. Chemical composition of AA7075, wt. %.

	Zn	Mg	Cu	Mn	Cr	Fe	Si	Al
AA7075	6.90	2.64	1.62	0.27	0.24	0.20	0.09	rest

SEM/EDS analysis of the aluminium alloy before testing in NaCl solution

The surface morphology and chemical composition of the polished 7075 aluminium alloy were analyzed by applying SEM/EDS. The 7075 aluminium alloy has a complex microstructure. In addition to strengthening precipitates of the nanometer size (GP zones and η` precipitates), this alloy contains intermetallic compounds (IMC) of the micrometre size that can be anodic or cathodic relative to the aluminium matrix (Fang et al. 2012; R. P. Wei, Liao, and Gao 1998).

Figure 2 presents SEM microphotographs of the 7075 aluminium alloy surface. Intermetallic compounds in the AA7075 alloy are seen as dark and light particles on the matrix area. The composition of the anodic and cathodic IMCs is analysed by the EDS and results are given in Table 2.

Anodic IMCs are darker than the aluminium matrix (Figure 2). EDS analysis showed that these IMCs are rich in Mg, Zn and Si (Spectrum 2, Table 2). Anodic IMCs dissolve in the initial period of the corrosion process and, due to their low dimensions, practically do not affect the corrosion properties of the examined aluminium alloy.

Cathodic IMCs are brighter than the aluminium matrix (Figure 2). They are rich in Fe and Cu, which is confirmed with EDS analysis (Spectrum 1, Table 2). During the corrosion process in a neutral NaCl solution, on the surface of the cathodic IMCs, the oxygen reduction reaction occurs. The presence of the cathodic IMCs on the surface of the aluminium alloy significantly decreased its corrosion properties. On the border of the cathodic IMCs occur different types of localized corrosion, such as pitting corrosion, intergranular corrosion etc.

Table 2. Results of EDS analysis of the 7075 aluminium alloy (from Figure 2) in mass. %

	Zn	Mg	Cu	Mn	Cr	Fe	Si	Al
Spectrum 1	2.0	0.0	3.5	5.1	2.3	16.3	4.3	Rest
Spectrum 2	9.3	7.7	2.1	0.0	0.4	0.0	2.1	Rest

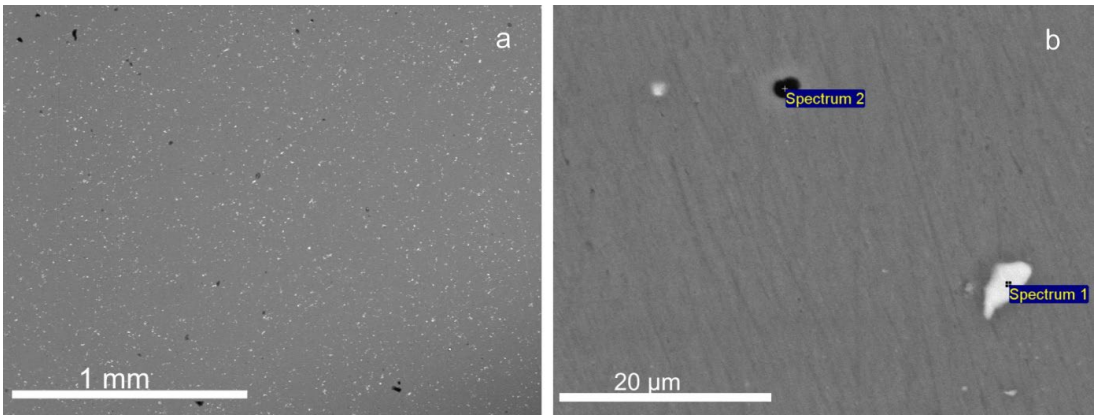

Fig. 2. SEM microstructure of 7075 aluminium alloy at different magnifications.

3.2. SEM analysis of the aluminium alloys after immersion in NaCl solution

The microstructure of the 7075 aluminium alloy after 24 h immersion in 0.1 M NaCl solution is analysed by SEM and a representative microphotograph is shown in Figure 3. Trenches along the edge of cathodic intermetallic compounds (IMCs) are visible. These trenches are formed in the presence of chloride ions, as a consequence of the anodic dissolution of the aluminium matrix in its vicinity, due to the potential difference between matrix and cathodic IMCs. The localized types of corrosion, such as pitting and intergranular corrosion, gradually form in places of formed trenches (Kappes et al. 2008; Goswami et al. 2013).

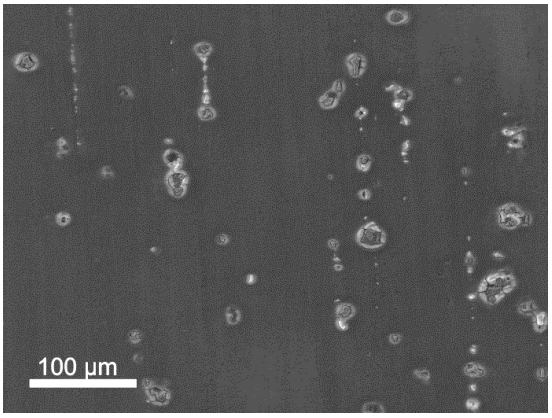

Fig. 3. SEM microphotograph of the 7075 aluminium alloy surface after 24 h of treatment in pure NaCl solution.

To protect the aluminium alloy surface from corrosion degradation, it is reasonable to use different protective strategies for corrosion protection. Using corrosion inhibitors is one of the simplest and most economical approaches.

3.3. Optimisation of corrosion inhibitor concentration

Determining the optimal concentration of inhibitor is a key step in researching the effects of corrosion protection. Using different electrochemical methods, the effectiveness of inhibitors (cystine and cysteine) in different concentrations was investigated. The linear polarization resistance (LPR) and electrochemical impedance spectroscopy (EIS) methods were applied. The LPR and EIS methods are the most commonly used non-destructive methods to investigate the efficiency of the inhibitors.

3.4. LPR method

Cysteine is an organic compound, and depending on the environment in which it is found, it can be an anodic, cathodic or mixed inhibitor (Raja et al. 2014). To determine the optimal amount of the inhibitors, several concentrations in the range of 0.03 mM – 0.1 mM of cysteine and cystine were tested for up to 72 h.

Figure 4 shows examples of the *E-j* polarization diagrams obtained by the LPR measurements, for the lowest (0.03 mM, Figure 4a) and the highest (0.1 mM, Figure 4b) concentrations of cysteine and cystine, after 24 hours of testing. The slope of the curves ($\Delta E/\Delta j$) on the corrosion potential corresponds to the values of polarization resistance (R_p).

The cystine has a higher value of polarisation resistance (R_p) than cysteine for all concentrations. Results of LPR measurements for tested inhibitors in different concentrations and at different times are given in Table 3.

Over time, a decrease in R_p value is observed for both inhibitors (Table 3). Generally, cystine showed a higher R_p value compared to cysteine during all tested periods.

After 24 h testing, the value of R_p increased with increasing concentration of cysteine. On the other hand, the reverse trend was observed with cystine (the value of R_p decreased with increasing concentration of cystine). This difference in the polarisation resistance

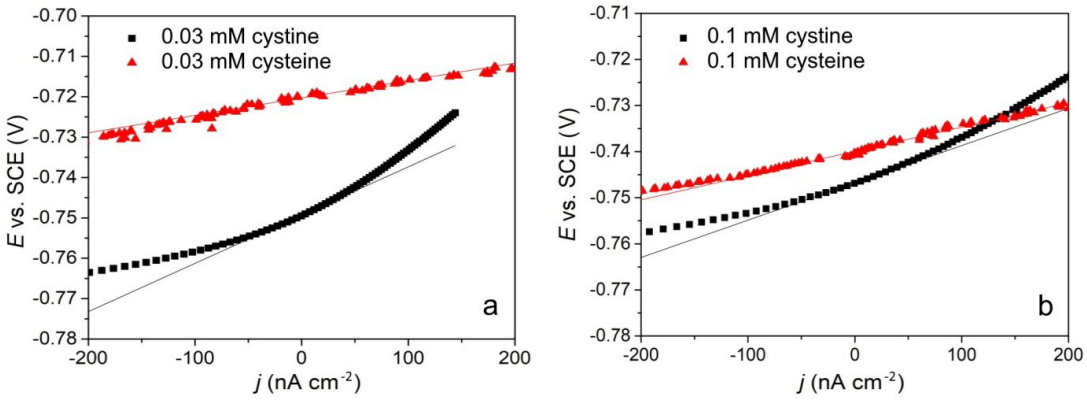

Fig. 4. LPR diagrams for different concentrations of cysteine and cysteine: a) 0.03 mM and b) 0.1 mM, after 24h.

between the two inhibitors suggests their different mechanisms of action.

Table 3. Values of polarization resistance (R_p) for different concentrations of cysteine and cystine, during different times on the 7075 aluminium alloy

Inhibitor	Time, h	Concentration, mM	Rp (kΩ cm²)
NaCl	24	0	5.51
	48		4.63
	72		3.79
cysteine + NaCl	24	0.03	42.8
	48		36.0
	72		29.9
	24	0.05	51.3
	48		32.6
	72		21.5
	24	0.10	53.4
	48		38.5
	72		24.8
cystine + NaCl	24	0.03	120
	48		98.9
	72		79.5
	24	0.05	96.3
	48		71.4
	72		67.5
	24	0.10	72.6
	48		70.5
	72		60.9

3.5. EIS method

To complete the results obtained by the LPR method, the EIS measurements were performed to evaluate the behaviour of both inhibitors in different concentrations. The obtained results are shown in Figure 5 and Table 4.

The diameter of the semicircle in the Nyquist plot (Figure 5) corresponds to the value of the polarization resistance. If the semicircle is incomplete, the polarization resistance value is determined by fitting the experimental data until the semicircle becomes well-defined. The fitting program provided by GAMRY potentiostat is used to analyze the experimental results.

The EIS results were analyzed using an Equivalent Electrical Circuit (EEC) with a one-time constant (Figure 6). The same EEC was applied to analyze the results of the aluminium alloy after treatment in pure NaCl solution. The EEC consists of electrolyte resistance (R_e), polarisation resistance (R_p) and constant phase element (CPE).

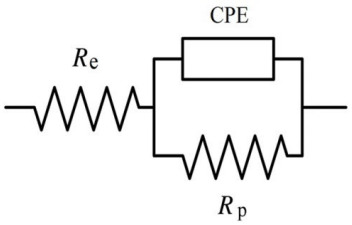

Fig. 6. Equivalent Electrical Circuit (EEC) used for EIS results analyte.

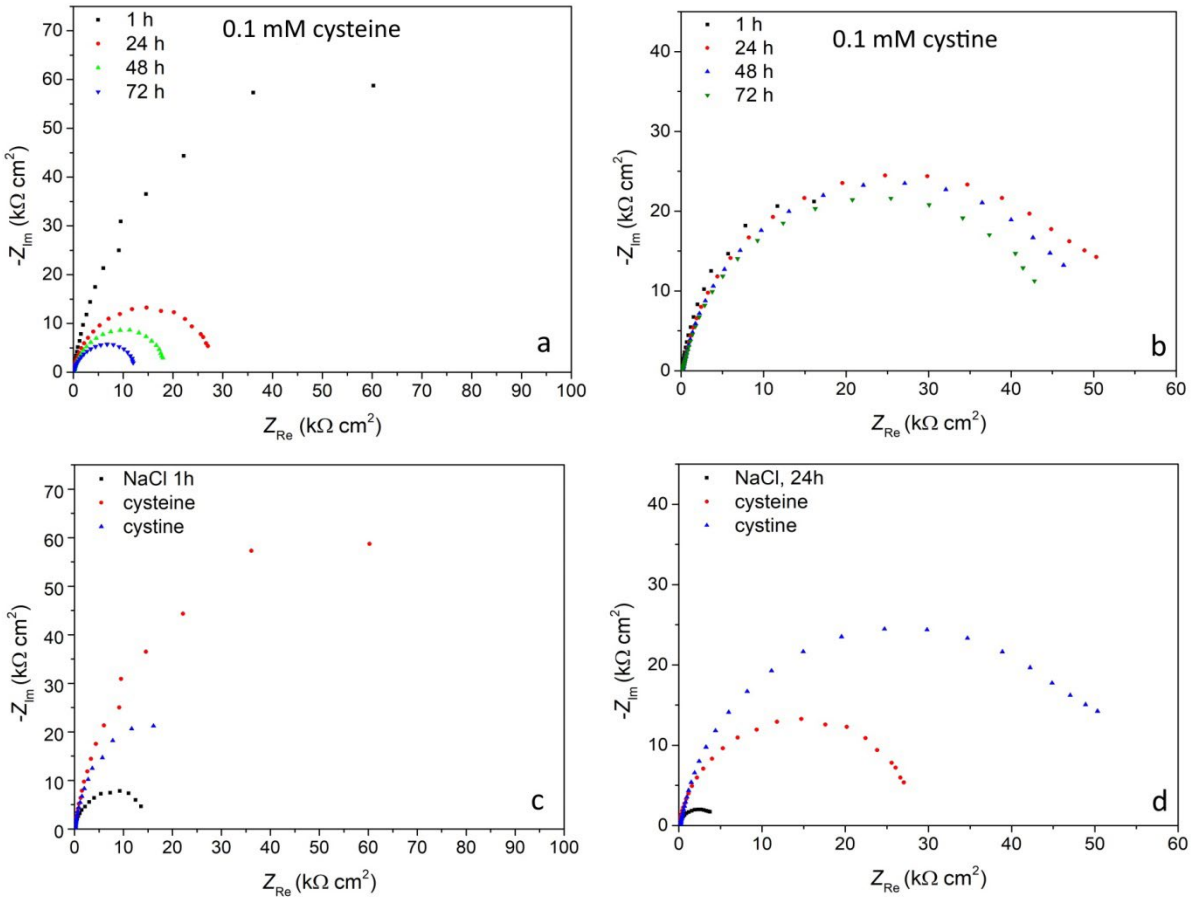

Fig. 5. Nyquist plots for different test times of: a) cysteine and b) cystine, c) 1 h test of cysteine and cystine, and d) 24 h test of cysteine and cystine in 0.1 M NaCl, on the 7075 aluminium alloy, at room temperature.

The constant phase element (CPE) is a complex quantity obtained by fitting the results obtained by EIS. The constant phase element consists of Yo and n. CPE includes all inhomogeneities of the metal surface and inhibitor layer. The value of the n indicates the difference Yo from ideal capacitance. For the ideal semicircle of the Nyquist diagram value of the n is equal to 1. The effective capacitance value (Ceff) is calculated using the following formula (Hirschorn et al. 2010):

$$C_{\text{eff}} = R_{\text{p}}^{\frac{1-n}{n}} \cdot Y_0^{\frac{1}{n}} \quad 7$$

For 24 h, 48 h and 72 h testing, cystine had a better efficiency compared to cysteine for all concentrations, while cystine for some reason showed to be a better inhibitor in the initial time of testing (1 h). It is possible that in the case of cysteine (which has a free -SH group), the direct binding of sulfur to the 7075 aluminium alloy surface occurred, already in the initial period of the test (1 h), thereby ensuring a higher value of polarization resistance (R_p). On the other hand, in the case of cystine, sulfur is bound in the -S-S- group, so it takes time to break the bond between the sulfur atoms and its binding to the surface of the aluminium alloy. Also, as a result of the breaking of the -S-S- bond, two cysteine molecules are obtained (each of which contains one atom of highly inhibitory effective sulfur), that is, twice the concentration of the inhibitor is obtained.

For further investigations, it was unnecessary to conduct experiments at all concentrations, as this is a comparative study. Therefore, a single concentration of 0.1 mM inhibitor was selected.

3.6. SEM analysis of the aluminium alloys after immersion in NaCl inhibitors solution

SEM analysis due to its limitations can not detect organic compounds on the surface of the examined specimen. Figure 7 shows the SEM microphotography of the aluminium alloy after immersion in a 0.1 M NaCl solution without and in the presence of the investigated corrosion inhibitors (cysteine and cystine). The surface of the aluminium alloy after 24 h immersion in a 0.1 M NaCl solution in the presence of cysteine was not affected by corrosion (Figure 7a), and its morphology looks like an untreated polished sample, as shown above in Figure 2. A thin layer of adsorbed cysteine, as an organic inhibitor, is not visible under the SEM microscope, but the undamaged surface of the aluminium alloy confirms the presence of the thin inhibitory layer. Also, in the case of the cystine, organic compounds on the surface of the examined specimen cannot be detected and a similar microstructure as with cysteine was obtained (Figure 7b).

Table 4. Data obtained by fitting the EIS diagram of cysteine and cystine depending on their concentration and time, on the 7075 aluminium alloy

Inhibitor	Time, h	Concentration, mM	Rp, kΩ cm²	CPE		Cef, μF cm⁻²
				Yo/10-6, s Ω⁻¹ cm⁻²	n	
NaCl	1	0	16.1	4.56	0.946	5.81
	24		5.51	26.4	0.895	47.4
	48		4.63	27.4	0.898	44.7
	72		3.79	45.0	0.882	89.6
NaCl + cysteine	1	0.03	120	5.04	0.901	10.2
	24		47.3	7.77	0.864	19.7
	48		29.6	8.98	0.867	21.2
	72		17.8	12.1	0.866	27.8
	1	0.05	296	4.43	0.940	7.01
	24		46.5	5.53	0.919	9.01
	48		22.5	7.65	0.899	13.6
	72		13.3	11.3	0.889	21.0
	1	0.10	150	5.37	0.916	9.91
	24		30.8	8.74	0.890	17.5
	48		20.1	11.2	0.880	23.4
	72		13.6	15.2	0.878	31.8
NaCl + cystine	1	0.03	89.8	4.86	0.937	7.31
	24		80.0	5.24	0.911	9.44
	48		41.6	5.60	0.903	10.1
	72		18.6	8.32	0.907	13.9
	1	0.05	257	4.22	0.934	6.92
	24		75.4	5.18	0.917	8.89
	48		60.0	5.54	0.908	9.98
	72		59.7	5.83	0.903	10.9
	1	0.10	72.6	4.70	0.929	7.33
	24		58.8	8.35	0.876	20.1
	48		57.7	9.69	0.859	27.4
	72		53.9	10.6	0.847	33.4

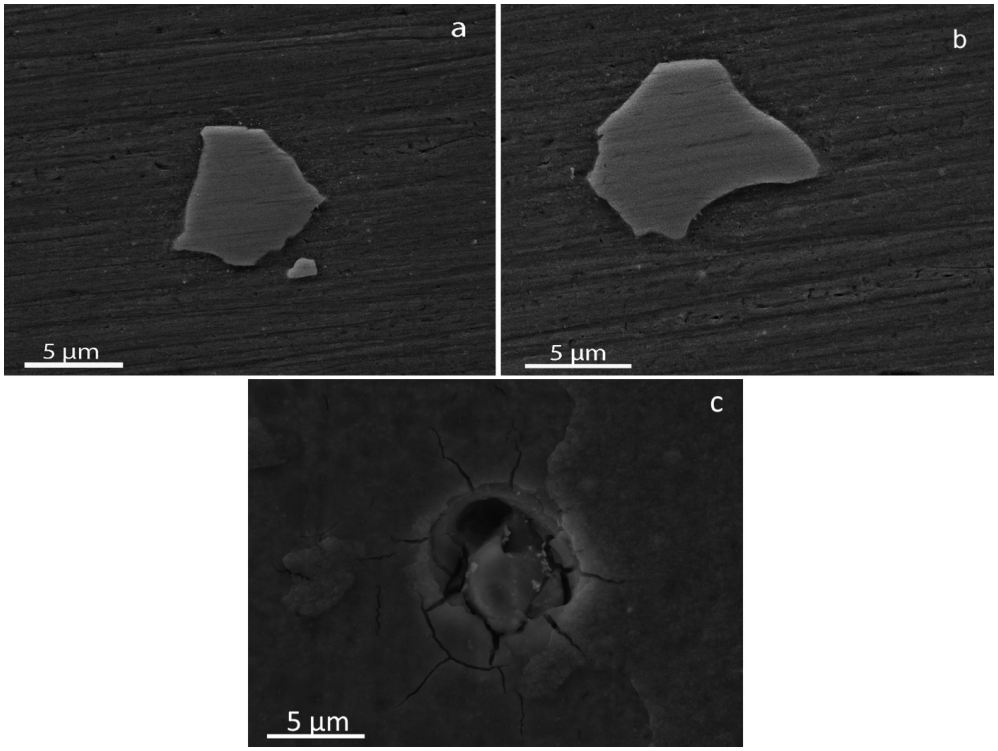

Fig. 7. SEM microphotograph of 7075 aluminium alloy after 24 h of treatment in 0.1 M NaCl solution in the presence of: a) 0.1 mM cysteine and b) 0.1 mM cysteine.

In the case of aluminium alloy after immersion in a 0.1 M NaCl solution without investigated inhibitors, trenches along the boundaries of cathodic IMCs are visible (Figure 7c). Localized corrosion types, such as pitting and intergranular corrosion, progressively develop in the areas where the trenches have formed (Kappes et al. 2008; Goswami et al. 2013).

3.7. Contact angle measurements of aluminium alloy after immersion in NaCl solution

To determine the degree of hydrophilicity of the inhibitor on the 7075 aluminium alloy, the contact angle was measured. Figure 8 shows specimens of the 7075 aluminium alloy immersed in a 0.1 M NaCl solution in the presence of the investigated corrosion inhibitors (cystine and cysteine). Table 5 shows the average value of the contact angle measured for all tested inhibitor systems.

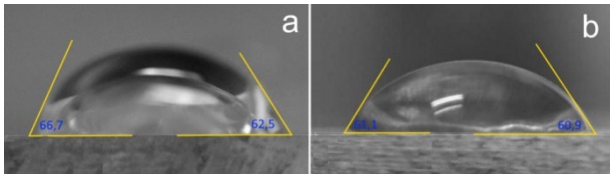

Fig. 8. Characteristic results of contact angle measurements on the tested aluminium alloy specimens after 24 h of treatment in 0.1 M NaCl solution in the presence of inhibitors: a) 0.1 mM cysteine and b) 0.1 mM cystine.

Table 5. Measured values of contact angle for tested inhibitor systems.

Solution	Contact angle, ^{o}
NaCl + cysteine	61.18 ± 4.26
NaCl + cystine	59.08 ± 4.97

Values of contact angle indicate the level of the surface hydrophilicity of the tested systems. Organic layers formed by cysteine and cystine have a similar impact on the surface properties which they cover. The values of the contact angle for cysteine and cystine are similar, although the contact angle for cysteine is a little higher. Cysteine had a value of ~ 61.2°, while cystine had a something lower value of ~ 59.1°. Probably, the value of the contact angle measurement is not a good enough indicator of the efficiency of the tested inhibitors on the aluminium alloy. Applied electrochemical methods, such as LPR and EIS are more appropriate indicators.

3.8. Appearance of specimens treated with NaCl inhibitors solution

The appearance of the 7075 aluminium alloy during 10 days of immersion in 0.1 M NaCl solution without and in the presence of the investigated corrosion inhibitors was recorded by applying an optical microscope (Figure 9).

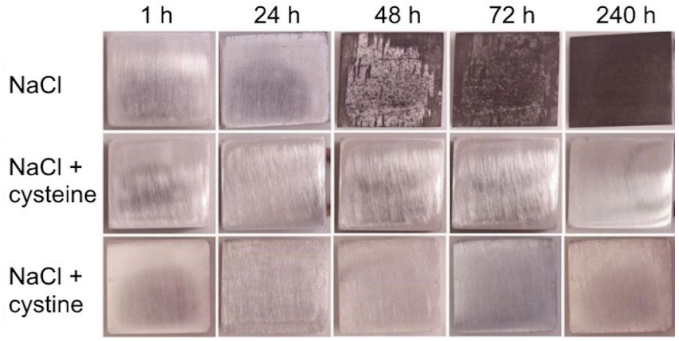

Fig. 9. Macro view of sample surfaces during 10 days of treatment in NaCl solution, without and in the presence of tested corrosion inhibitors, at room temperature.

The aluminium alloy specimens immersed in NaCl solution without inhibitors begin to corrode yet after 24 h. After 48 h of testing on the specimen surface, high corrosion degradation is visible, due to the occurrence of different types of corrosion reactions, as discussed above. After 10 days of immersion, the specimen surface was completely covered with corrosion products. In contrast, the aluminium alloy specimens that were immersed in the inhibitor solution remained undamaged, i.e. even after 10 days in the inhibitor solution there were no visible changes

Table 6. Data obtained by fitting EIS diagrams of cysteine and cystine depending on temperature, on 7075 aluminium alloy

Solution	t, °C	Rp, kΩ cm²	CPE		Cef, μF cm⁻²	IE, %
			Yo/10⁻⁶, s Ω⁻¹ cm⁻²	n		
NaCl	20	16.1	4.56	0.946	5.81	/
	30	3.97	9.13	0.930	7.11	/
	40	2.94	12.9	0.917	9.56	/
NaCl + cysteine	20	150	5.37	0.916	4.80	89.3
	30	252	4.95	0.913	5.06	98.4
	40	188	5.18	0.911	5.17	98.4
NaCl + cystine	20	72.6	4.70	0.929	7.33	77.8
	30	49.4	5.80	0.956	5.48	92.0
	40	34.1	7.44	0.936	6.78	91.4

on the metal surface. Although macro surface changes were not visible, it does not mean that corrosion damage on the micro level to a lesser extent was not present.

3.9. *The effectiveness of corrosion inhibitors dependence on temperature and their thermodynamics Kinetics*

The effectiveness of the corrosion inhibitors dependence on the temperature was studied using the EIS method. The inhibitory efficiency of cysteine (0.1 mM) and cystine (0.1 mM) was tested after 1 h in a 0.1 M NaCl solution in the temperature range from 20 to 40 °C. The obtained results for the solution without and in the presence of inhibitors are shown in Table 6.

The efficiency of cystine and cysteine inhibitors have significantly higher value compared to the NaCl solution without inhibitors, for all temperatures. This indicates that the inhibitor molecules are adsorbed on the aluminium alloy surface, even at room temperature. Also, the obtained results are in agreement with the results of previous electrochemical measurements. Cysteine, after 1 h of testing, had a better inhibitory efficiency compared to cystine, as discussed above.

Using the Arrhenius equation (3), the activation energy Ea and the pre-exponential factor A were calculated for 0.1 M NaCl solution in the presence of the investigated corrosion inhibitors (cysteine and cystine). The corrosion rate (CR) is calculated using the expression CR=B/Rp and depends on the temperature ln(CR) = f(1/T). B is a constant and its value is taken from the literature and is 26 mV (Baboian and Treseder, 2002).

Figure 10 shows the graphical dependence of $\ln(C_R)$ - *1/T,* where $-E_a/R$ is the slope of the line, and the ln*A* is the intercept. The obtained values of E_a and *A* are given in Table 7.

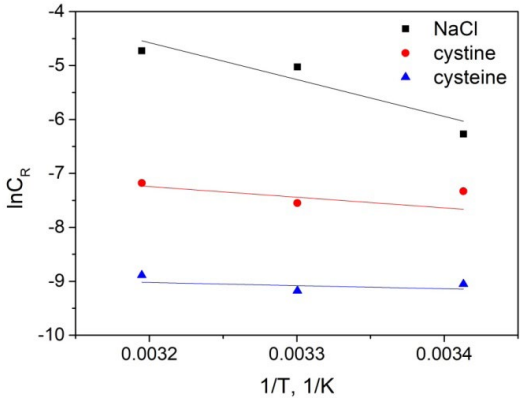

Fig. 10. Arrhenius dependence of the logarithm of the corrosion inhibitor concentration on the reciprocal of temperature.

Based on electrochemical measurements at different temperatures, in addition to the activation energy (E_a) and the pre-exponential factor (*A*), other kinetic parameters were calculated: activation entropy (ΔS°) and activation enthalpy (ΔH°), using Equation (2). The obtained results are given in Table 7. Using the graph $ln(C_R)$ - *1/T,* the values of ΔH° and ΔS° were calculated. This graphical dependence is a straight line with slope $-\Delta N/R$ and intercept .

Table 7. Kinetic parameters E_a, ΔH° and ΔS° for the aluminium alloy in 0.1 M NaCl solution in the presence of corrosion inhibitors.

Solution	E_a, kJ/mol	*A*, μA cm²	ΔS°, J/molK	ΔH°, kJ/mol
NaCl	56.9	$3.27 \cdot 10^{11}$	-73.6	24.9
NaCl + cysteine	4.83	$4.00 \cdot 10^{3}$	-103	1.06
NaCl + cystine	16.4	7.75	-143	6.39

A lower value of the pre-exponential factor (*A*) indicates that a reaction is less likely to occur (Nakomčić 2016). This means a lower corrosion current density (j_{corr}), (according to Equation (1)), and consequently a lower corrosion rate (C_R) can be expected. A lower value of *A* indicates a lower frequency of collisions leading to a corrosion reaction, which means that corrosion is slower or less likely under the given conditions.

A positive enthalpy value ($\Delta H^\circ > 0$) indicates an endothermic process of metal dissolution in the presence and absence of inhibitors (Okewale and Adesina 2020; Singh and Quraishi 2010). In all cases (Table 7), the ΔH° value is positive. Also, a lower ΔH° value was obtained for cysteine than for cystine.

A negative entropy value ($\Delta S^\circ < 0$) indicates a reduction in the disorder of the system during corrosion (Fu et al. 2011). In all cases, the value of ΔS° is negative, and a more negative value means that the system is more organized and that the chance for corrosion to occur is lower. Lower values of entropy were obtained in inhibitive solutions than in NaCl solution without inhibitor (Table 7).

3.10. *Adsorption isotherm*

The inhibitor effectiveness of cysteine and cystine was also studied as a function of concentration, at different times, using the EIS method. The obtained results for the solution without and in the presence of inhibitors are shown in Table 8. Inhibitor effectiveness (IE%) decreased over time, for both inhibitors in all concentrations. Values of Rp are obtained by fitting the EIS results, using the EEC with a one-time constant (Figure 6), while IE is recalculated from the Equation:

$$IE = \frac{R_{p,inh} - R_{p,0}}{R_{p,inh}} \cdot 100\% \qquad 8$$

Where, $R_{p,inh}$ is the polarisation resistance of inhibitor solution, and $R_{p,o}$ is the polarisation resistance of inhibitor-free solution (0.1M NaCl).

Table 8. Values of polarization resistance depending on the time of exposure to 0.1 M NaCl solution, for different inhibitor concentrations (cysteine and cystine).

Solution	C, mM	R_p, kΩ cm²				*I.E.*, %			
		1 h	24 h	48 h	72 h	1 h	24 h	48 h	72 h
NaCl	0	16.1	5.47	4.63	3.79	/	/	/	/
NaCl + cysteine	0.03	120	47.3	29.6	17.8	86.6	88.4	84.4	78.7
	0.05	296	46.5	22.2	13.2	94.6	88.2	79.1	71.3
	0.10	150	30.8	20.1	13.6	89.3	82.2	76.9	72.1
NaCl + cystine	0.03	89.8	80.0	41.6	18.6	82.1	93.2	88.9	79.6
	0.05	257	75.4	60.0	59.7	93.7	92.7	92.3	93.7
	0.10	72.6	58.8	57.7	53.9	77.8	90.7	92.0	93.0

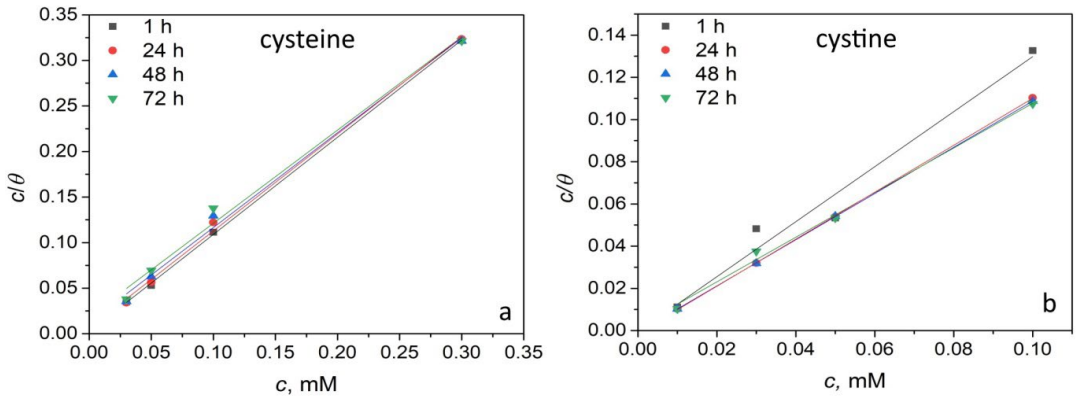

Fig. 11. Langmuir adsorption isotherms for a) cysteine and b) cystine.

Figure 11 shows the Langmuir adsorption isotherm for cysteine and cystine during the 72 h test of the 7075 aluminium alloy specimens.

With the increase in concentration, the ratio c/θ increases for all tested times. Table 9 shows the values of K_{ads} for cysteine and cystine inhibitors during different periods. Based on this it can be seen that K_{ads} decreases with time. It is generally known that the adsorption constant indicates the adsorption power of the inhibitor on the surface of the metal, in this case on the surface of the 7075 aluminium alloy (Li et al. 2014; Bahaa Sami Mahdi et al. 2016).

Table 9. Parameters of graphical dependence $c/\theta - c$, for different times in the presence of cysteine and cystine corrosion inhibitors.

Inhibitor	Time, h	K, mM^{-1}	K_{ads}
cysteine	1 h	444.4	24664.2
	24 h	158.2	8780.10
	48 h	80.45	4464.98
	72 h	52.94	2938.17
cystine	1 h	1812	100566
	24 h	819.7	45493.4
	48 h	1376	76368.0
	72 h	515.5	28610.3

The adsorption constant (K_{ads}) decreased during time, for both tested inhibitors (Table 9). This means that inhibitive efficiency decreased over time. Also, value K_{ads} for cystine generally has a higher value than for cysteine.

3.11. Thermodynamic parameters of inhibitor adsorption

The equilibrium constant of the adsorption process is related to the thermodynamic parameter of the standard Gibbs free energy of adsorption (ΔG_{ads}) according to the equation:

$$\Delta G_{ads}^{o} = \Delta H_{ads}^{o} - T\,\Delta S_{ads}^{o} \quad (9)$$

The obtained values for ΔG_{ads} are shown in Table 10. The negative value of ΔG_{ads} (Table 10) means that the thermodynamic process of adsorption is favourable. Over time, ΔG_{ads} becomes less negative for both inhibitors, which may indicate a decrease in adsorption efficiency i.e. change in the interactions between the inhibitor and the alloy surface.

Table 10. Thermodynamic parameters for different concentrations of cysteine and cystine determined after different times of testing.

Inhibitor	Time, h	K_{ads}	ΔG_{ads}, kJ/mol
cysteine	1 h	24664.2	-24.80
	24 h	8780.10	-22.27
	48 h	4464.98	-20.61
	72 h	2938.17	-19.58
cystine	1 h	100566	-28.25
	24 h	45493.4	-26.31
	48 h	76368.0	-27.58
	72 h	28610.3	-25.19

Adsorption of inhibitor molecules to the metal surface can have a physical character (relatively weak attractive forces between the inhibitor molecules and the metal surface), a chemical character (strong attractive forces between the inhibitor molecules and the metal surface) and a mixed character. In physical adsorption, the attraction between inhibitor molecules and the surface of the metal occurs as a result of their different (opposite) charges. In chemical adsorption, chemical bonds are formed between inhibitor molecules and the metal surface. It is usually considered that, if the value of ΔG_{ads} is more negative than -40 kJ/mol, then the adsorption is chemical. When the value of ΔG_{ads} is more positive than -20 kJ/mol, then adsorption can be considered as physical adsorption, and for values of ΔG_{ads} between -40 kJ/mol and -20 kJ/mol, adsorption has a mixed character (Fragoza-Mar et al. 2012). In the considered case (Table 10), the obtained ΔG_{ads} values were between -20 kJ/mol and -40 kJ/mol, so it can be considered that the adsorption of the cysteine and cystine inhibitors on the surface of the tested aluminium alloy is mixed (physical and chemical).

Overall, the present results show that cystine provides longer-lasting corrosion protection compared to cysteine. Although cysteine quickly creates a protective film thanks to the free thio group, cystine, due to the disulfide bond (which probably breaks during time), shows a slower onset of adsorption, but at the same time provides a more stable protective layer over a longer period.

4. Conclusin

Based on the presented results, it can be concluded that cysteine and cystine are effective corrosion inhibitors for the 7075 aluminium alloy in 0.1M NaCl solution. Their effectiveness differs, depending on the applied conditions.

The presence of anodic and cathodic intermetallic compounds (IMCs) on the surface of the aluminium alloy was confirmed by SEM/EDS analysis. Cathodic IMCs are prone to trench and pit formation.

The addition of inhibitors (cysteine and cystine) significantly reduced trench formation and consequently pitting corrosion occurrence and formation of the pits.

Cysteine exhibits superior protective ability in the initial period of testing, while cystine is more effective in long-term applications. An explanation of this behaviour is proposed in the manuscript.

Thermodynamic and kinetic parameters indicate that cysteine and cystine are adsorbed on the metal surface, reducing the surface energy and preventing corrosion processes. Values ΔG_{ads} are between -20 kJ/mol and -40 kJ/mol, which means that the adsorption of inhibitors for the aluminium alloy surface has a mixed physical and chemical character.

Acknowledgements

This study was financially supported by the Ministry of Education, Science and Technological Development of the Republic of Serbia (Grant No. 451-03-47/2023-01/200026 and 451-03-66/2024-03/200023).

Declarations Conflict of interest

The authors have no financial or proprietary interests in any material discussed in this article.

References

Abd El Haleem, S. M., S. Abd El Wanees, E. E. Abd El Aal, and A. Farouk. 2013. “Factors Affecting the Corrosion Behaviour of Aluminium in Acid Solutions. I. Nitrogen and/or Sulphur-Containing Organic Compounds as Corrosion Inhibitors for Al in HCl Solutions.” *Corrosion Science* 68: 1–13. https://doi.org/10.1016/j.corsci.2012.03.021.

Andreatta, F., H. Terryn, and J. H.W. De Wit. 2004. “Corrosion Behaviour of Different Tempers of AA7075 Aluminium Alloy.” *Electrochimica Acta* 49 (17–18): 2851–62. https://doi.org/10.1016/j.electacta.2004.01.046.

B. A. ABD-E1-NABEY, N. KHALIL and A. MOHAMED. 1985. “Inhibition by Amino Acids of the Corrosion of Steel in Acid.” *Surface Technology* 24: 383–89.

Baboian, Robert, and R.S. Treseder. n.d. “CORROSION ENGINEER ’ S REFERENCE Third Edition.”

Bahaa Sami Mahdi, Muna Khethier Abbass, Mustafa Khudhair Mohsin, Waleed Khalid Al-azzawi, Mahdi M. Hanoon, Mohammed Hliyil Hafiz Al-kaabi, Lina M. Shaker, Ahmed A. Al-amiery, and Abdul Amir H. Kadhum and Mohd S. Takriff , Wan Nor Roslam Wan Isahak. 2016. “Corrosion Inhibition of Mild Steel in Hydrochloric Acid Using4-(Pyridin-2yl)-N-p-Tolylpiperazine-1-Carboxamide.” *International Journal of Electrochemical Science* 11 (5): 3393–3414. https://doi.org/10.20964/10109.

Constable, David J.C., Alan D. Curzons, and Virginia L. Cunningham. 2002. “Metrics to ‘green’ Chemistry - Which Are the Best?” *Green Chemistry* 4 (6): 521–27. https://doi.org/10.1039/b206169b.

Costa, Max, and Catherine B. Klein. 2006. “Toxicity and Carcinogenicity of Chromium Compounds in Humans.” *Critical Reviews in Toxicology* 36 (2): 155–63. https://doi.org/10.1080/10408440500534032.

“Directive (EU) 2022/431 of the European Parliament and of the Council of 9 March 2022 Amending Directive 2004/37/EC on the Protection of Workers from the Risks Related to Exposure to Carcinogens or Mutagens at Work.” 2022.

Fang, Xu, Min Song, Kai Li, Yong Du, Dongdong Zhao, Chao Jiang, and Hong Zhang. 2012. “Effects of Cu and Al on the Crystal Structure and Composition of η (MgZn 2) Phase in over-Aged Al-Zn-Mg-Cu Alloys.” *Journal of Materials Science* 47 (14): 5419–27. https://doi.org/10.1007/s10853-012-6428-9.

Fragoza-Mar, Lubanski, Octavio Olivares-Xometl, Marco A. Domínguez-Aguilar, Eugenio A. Flores, Paulina Arellanes-Lozada, and Federico Jiménez-Cruz. 2012. “Corrosion Inhibitor Activity of 1,3-Diketone Malonates for Mild Steel in Aqueous Hydrochloric Acid Solution.” *Corrosion Science* 61: 171–84. https://doi.org/10.1016/j.corsci.2012.04.031.

Fu, Jiajun, Junyi Pan, Zhuo Liu, Suning Li, and Ying Wang. 2011. “Corrosion Inhibition of Mild Steel by Benzopyranone Derivative in 1.0 M HCl Solutions.” *International Journal of Electrochemical Science* 6 (6): 2072–89. https://doi.org/10.1016/s1452-3981(23)18168-5.

Goswami, Ramasis, Stanley Lynch, N. J.Henry Holroyd, Steven P. Knight, and Ronald L. Holtz. 2013. “Evolution of Grain Boundary Precipitates in Al 7075 upon Aging and Correlation with Stress Corrosion Cracking Behavior.” *Metallurgical and Materials Transactions A: Physical Metallurgy and Materials Science* 44 (3): 1268–78. https://doi.org/10.1007/s11661-012-1413-0.

Hirschorn, Bryan, Mark E. Orazem, Bernard Tribollet, Vincent Vivier, Isabelle Frateur, and Marco Musiani. 2010. “Constant-Phase-Element Behavior Caused by Resistivity Distributions in Films.” *Journal of The Electrochemical Society* 157 (12): C458. https://doi.org/10.1149/1.3499565.

Hluchan, V., B. L. Wheeler, and N. Hackerman. 1988. “Amino Acids as Corrosion Inhibitors in Hydrochloric Acid Solutions.” *Materials and Corrosion* 39 (11): 512–17. https://doi.org/10.1002/maco.19880391106.

Ibrahimi, Brahim El, Aziz Jmiai, Aziza Somoue, Rachid Oukhrib, Mohamed Chadili, Souad El Issami, and Lahcen Bazzi. 2018. “Cysteine Duality Effect on the Corrosion Inhibition and Acceleration of 3003 Aluminium Alloy in a 2% NaCl Solution.” *Portugaliae Electrochimica Acta* 36 (6): 403–22. https://doi.org/10.4152/pea.201806403.

Kappes, M., L. Kovarik, M. J. Mills, G. S. Frankel, and M. K. Miller. 2008. “Usefulness of Ultrahigh Resolution Microstructural Studies for Understanding Localized Corrosion Behavior of Al Alloys.” *Journal of The Electrochemical Society* 155 (8): C437. https://doi.org/10.1149/1.2939212.

Kokalj, Anton. 2023. “On the Use of the Langmuir and Other Adsorption Isotherms in Corrosion Inhibition.” *Corrosion Science* 217 (December 2022): 111112. https://doi.org/10.1016/j.corsci.2023.111112.

Li, Xianghong, Xiaoguang Xie, Shuduan Deng, and Guanben Du. 2014. “Two Phenylpyrimidine Derivatives as New Corrosion Inhibitors for Cold Rolled Steel in Hydrochloric Acid Solution.” *Corrosion Science* 87: 27–39. https://doi.org/10.1016/j.corsci.2014.05.017.

M. O. Speidel, M. V. Hyatt. 1972. *In Advances in Corrosion Science and Technology*. Edited by R. W. Staehle M. G. Fontana. Vol 2. London, NewYork: Plenum Press,.

Mars G. Fontana. 1987. *Corrosion Engineering and Corrosion Science. Materials Performance*. Third. McGraw-Hill Book Company. https://doi.org/10.5006/0010-9312-19.6.199.

Milošev, Ingrid, Jasminka Pavlinac, Milan Hodošček, and Antonija Lesar. 2013. “Amino Acids as Corrosion Inhibitors for Copper in Acidic Medium: Experimental and Theoretical Study.” *Journal of the Serbian Chemical Society* 78 (12): 2069–86. https://doi.org/10.2298/JSC131126146M.

Morad, M. S. 2008. “Corrosion Inhibition of Mild Steel in Sulfamic Acid Solution by S-Containing Amino Acids.” *Journal of Applied Electrochemistry* 38 (11): 1509–18. https://doi.org/10.1007/s10800-008-9595-2.

Nakata, Kazuhiro, Young Gon Kim, Masao Ushio, Takenori Hashimoto, and Shigetoshi Jyogan. 2000. “Weldability of High Strength Aluminum Alloys by Friction Stir Welding.” *ISIJ International* 40 (SUPPL.). https://doi.org/10.2355/isijinternational.40.suppl_s15.

Nakomčić, Jelena. 2016. “Proučavanje Korozije Bakra u Prisustvu Odabranih Derivata Tiazola.” UNIVERZITET U NOVOM SADU PRIRODNO-MATEMATIČKI FAKULTET DEPARTMAN ZA HEMIJU, BIOHEMIJU I ZAŠTITU ŽIVOTNE SREDINE.

Okewale, A.O., and O.A. Adesina. 2020. “Kinetics and Thermodynamic Study of Corrosion Inhibition of Mild Steel in 1.5m HCl Medium Using Cocoa Leaf Extract as Inhibitor.” *Journal of Applied Sciences and Environmental Management* 24 (1): 37. https://doi.org/10.4314/jasem.v24i1.6.

Raja, A Sahaya, R Venkatesan, R Sonisheeba, J Thomas Paul, S Sivakumar, P Angel, and J Sathiyabama. 2014. “Corrosion Inhibition by Cysteine - An Over View.” *International Journal of Advanced Research in Chemical Science* 1 (1): 101–9.

Saifi, H., M. C. Bernard, S. Joiret, K. Rahmouni, H. Takenouti, and B. Talhi. 2010. “Corrosion Inhibitive Action of Cysteine on Cu-30Ni Alloy in Aerated 0.5 M H2SO4.” *Materials Chemistry and Physics* 120 (2–3): 661–69. https://doi.org/10.1016/j.matchemphys.2009.12.011.

Shinato, Kebede W., Feifei Huang, Yanpeng Xue, Lei Wen, and Ying Jin. 2019. “The Protection Role of Cysteine for Cu-5Zn-5Al-1Sn Alloy Corrosion in 3.5 Wt.% NaCl Solution.” *Applied Sciences (Switzerland)* 9 (18). https://doi.org/10.3390/app9183896.

Singh, Ashish Kumar, and M. A. Quraishi. 2010. “Effect of Cefazolin on the Corrosion of Mild Steel in HCl Solution.” *Corrosion Science* 52 (1): 152–60. https://doi.org/10.1016/j.corsci.2009.08.050.

Swatloski, Richard P., Scott K. Spear, John D. Holbrey, and Robin D. Rogers. 2002. “Dissolution of Cellose with Ionic Liquids.” *Journal of the American Chemical Society* 124 (18): 4974–75. https://doi.org/10.1021/ja025790m.

Tawfik, Salah M. 2015. “Corrosion Inhibition Efficiency and Adsorption Behavior of N,N-Dimethyl-4-(((1-Methyl-2-Phenyl-2,3-Dihydro-1H-Pyrazol-4-Yl)Imino) Methyl)-N-Alkylbenzenaminium Bromide Surfactant at Carbon Steel/Hydrochloric Acid Interface.” *Journal of Molecular Liquids* 207: 185–94. https://doi.org/10.1016/j.molliq.2015.03.036.

Uhlig, H. H., and R. W. Revie. 1985. *Corrosion and Corrosion Control. An Introduction to Corrosion Science and Engineering. Third Edition*.

V.S Sinjavskij, V.D. Valjkov, V.D. Kalinin. 1986. "Corrosion and Protection of Aluminium Alloys." *Metallurgia*.

Vargel, Christian. 2004. "The Metallurgy of Aluminium." In *Corrosion of Aluminium*, 23–57. https://doi.org/10.1016/b978-008044495-6/50008-2.

Wei, L. L., Q. L. Pan, L. Feng, Y. L. Wang, and H. F. Huang. 2015. "Effect of Aging on Corrosion Property, Electrochemical Behavior and Microstructure of Al-Zn-Mg-Cu Alloy." *Materials and Corrosion* 66 (1): 54–60. https://doi.org/10.1002/maco.201307095.

Wei, Robert P., Chi Min Liao, and Ming Gao. 1998. "A Transmission Electron Microscopy Study of Constituent-Particle-Induced Corrosion in 7075-T6 and 2024-T3 Aluminum Alloys." *Metallurgical and Materials Transactions A: Physical Metallurgy and Materials Science* 29 (4): 1153–60. https://doi.org/10.1007/s11661-998-0241-8.

Zhang, Bingru, Chengjun He, Cheng Wang, Peidi Sun, Fengting Li, and Yu Lin. 2015. "Synergistic Corrosion Inhibition of Environment-Friendly Inhibitors on the Corrosion of Carbon Steel in Soft Water." *Corrosion Science* 94: 6–20. https://doi.org/10.1016/j.corsci.2014.11.035.

Zhang, Pandong, Liang He, Xiaolu Sun, Xinran Liu, and Ping Li. 2023. "Study on the Inhibitory Effect of Cystine, Cysteine, and Clutamate as Inhibitors on X100 Pipeline Steel in 1 M HCl." *Electrocatalysis* 14 (5): 720–31. https://doi.org/10.1007/s12678-023-00830-1.